

Representation-Aware Unlearning via Activation Signatures: From Suppression to Knowledge-Signature Erasure

Syed Naveed Mahmood¹, Md. Rezaur Rahman Bhuiyan^{1*}, Tasfia Zaman^{1*}, Jareen Tasneem Khondaker¹, Md. Sameer Sakib¹, Nazia Tasnim², Farig Sadeque¹

¹Computer Science and Engineering, BRAC University, Dhaka, Bangladesh

²Boston University, Boston, MA, USA

*Equal contribution.

Abstract

Selective knowledge erasure from LLMs is critical for GDPR compliance and model safety, yet current unlearning methods conflate behavioral suppression with true knowledge removal, allowing latent capabilities to persist beneath surface-level refusals. In this work, we address this challenge by introducing **Knowledge Immunization Framework (KIF)**, a representation-aware architecture that distinguishes genuine erasure from obfuscation by targeting internal activation signatures rather than surface outputs¹. Our approach combines dynamic suppression of subject-specific representations with parameter-efficient adaptation, enabling durable unlearning without full model retraining. KIF achieves near-oracle erasure ($FQ \approx 0.99$ vs. 1.00) while preserving utility at oracle levels ($MU = 0.62$), effectively breaking the stability-erasure tradeoff that has constrained all prior work. We evaluate both standard foundation models (Llama & Mistral) and reasoning-prior models (Qwen & DeepSeek) across 3B to 14B parameters. Our observation shows that standard models exhibit scale-independent true erasure (<3% utility drift), while reasoning-prior models reveal fundamental architectural divergence. Our comprehensive dual-metric evaluation protocol, combining surface-level leakage with latent trace persistence, operationalizes the obfuscation - erasure distinction and enables the first systematic diagnosis of mechanism-level forgetting behavior across model families and scales.

1 Introduction

Large language models (LLMs) are widely deployed in NLP systems, but training on large-scale corpora can memorize sensitive or copyrighted content, conflicting with regulations such as the GDPR (European Parliament and Council of the European Union, 2016) “right to erasure” / right to be forgotten (RTBF) and related data-protection regimes

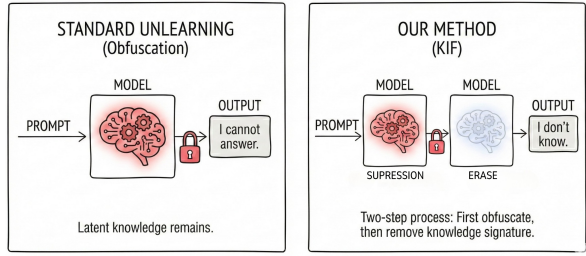


Figure 1: **Comparison of approaches**: while standard methods may yield obfuscation that hides answers without removing latent knowledge, KIF targets the internal signature to achieve true erasure.

(Zhang et al., 2024a). Unlike databases, where deletion is explicit, LLMs entangle training data in distributed parameters (Naveed et al., 2025), making targeted removal technically difficult. *LLM unlearning* aims to remove the influence of selected data while preserving general utility (Yao et al., 2024; Ren et al., 2025). Recent unlearning methods include reverse-optimization (e.g., gradient ascent (Yao et al., 2024)), preference-based objectives such as NPO (Zhang et al., 2024b), and representation-steering approaches (RMU (Hu-Tien et al., 2025), Opt-Out (Choi et al., 2025)). Despite efficiency, two primary issues persist: (i) utility can degrade under strong forgetting pressure (Yao et al., 2024; Zhang et al., 2024b); (ii) apparent forgetting can be obfuscation (refusal/suppression) rather than erasure, leaving latent capability intact (Ren et al., 2025; Sun et al., 2025).

We address these limitations by proposing **Knowledge Immunization Framework (KIF)**: a light-weight framework that uses internal representation signals, extracted using a custom real-world entity based prompt dataset, to target the knowledge to dynamically suppress output during inference, continually distill the suppression into parameter weights using LoRA (Hu et al., 2021): unlearning it while applying stability-aware updates to reduce collateral drift, discouraging obfuscation.

¹Anonymous repository

We evaluate across open-source chat and reasoning model families across varying scales using benchmarks and metrics that probe both surface leakage and residual knowledge (Maini et al., 2024; Shi et al., 2024; Yoon et al., 2025). **KIF** achieves strong forgetting with negligible utility drift in foundation models and exposes systematic differences in how reasoning-oriented models trade off erasure and obfuscation under stress (Sun et al., 2025; Yoon et al., 2025). Our main contributions can be summarized as: **(i)** a custom real-world entity based prompt dataset; **(ii)** a representation-aware, dynamic suppression and parameter-efficient unlearning framework guided by internal activation signatures based on the dataset, improving stability over standard baselines; **(iii)** an evaluation protocol that separates behavioral suppression from durable erasure by jointly measuring leakage and internal signature persistence; **(iv)** a cross-family, cross-scale study identifying regimes where unlearning remains stable versus regimes that revert to obfuscation-like behavior under pressure.

2 Related Works

Most practical LLM unlearning avoids expensive retraining by optimizing auxiliary objectives on a *forget* set while preserving utility, with TOFU (Maini et al., 2024) and MUSE (Shi et al., 2024) establishing standard benchmarks. Early approaches, such as reverse-optimization baselines like Maini et al. (2024), regularize forgetting against retention, while preference-style objectives (Zhang et al., 2024b; Rafailov et al., 2024) such as NPO (Zhang et al., 2024b) provide smoother divergence than Jang et al. (2023). Subsequent work has progressively addressed stability and failure modes: Fan et al. (2025) reduces reference bias, AltPO (Mekala et al., 2025) incorporates in-domain positives, ReLearn (Xu et al., 2025) preserves fluency through learning-style updates, and UNDIAL (Dong et al., 2025) applies self-distillation-based stabilization. Optimizer/geometry choices (SOUL (Jia et al., 2024)) and robustness to relearning attacks via smoothness-aware defenses (e.g., SAM-based (Fan et al., 2025) robust unlearning) further shape outcomes. Despite these refinements, a fundamental issue persists: existing methods operate at the loss and output levels, treating forgetting as a behavioral adjustment rather than a representation-level phenomenon. This architectural choice leaves a critical gap: apparent forget-

ting often masks *obfuscation* (i.e, suppression vs. refusal) rather than true knowledge erasure.

Recent work has begun to expose this gap. Sun et al. (2025) and Yoon et al. (2025) demonstrate that obfuscation can hide residual knowledge through probing-based evaluations and that reasoning models are particularly susceptible, leaving intermediate traces despite answer-level suppression. Parameter-efficient methods like LoRA (Hu et al., 2021; Liu et al., 2022) and mechanistic approaches localizing knowledge in transformer internals (e.g., knowledge neurons, activation patching (Dai et al., 2022; Heimersheim and Nanda, 2024) offer complementary insights, yet neither directly targets the obfuscation - erasure distinction. We bridge these directions by mining forget-linked activation signatures to guide localized PEFT edits, combining representation-aware intervention with parameter efficiency while explicitly measuring both surface behavior and latent persistence.

3 Methodology

To achieve our goal of a durable, representation-level knowledge erasure while preserving model utility, we introduce a three-stage pipeline: **(1)** *localizing* the target knowledge’s internal activation mechanisms through statistical analysis (Meng et al., 2023), **(2)** then *suppressing* these mechanisms at inference time using lightweight gating modules termed **Knowledge Suppression Capsules** to attenuate subject-specific representations, and **(3)** finally, *distilling* this suppressed behavior permanently into a global LoRA Adapter (Hu et al., 2021) for durable unlearning without full retraining. The training objective combines preference-style supervision for explicit forgetting and stability regularization that minimize collateral drift (Rafailov et al., 2024; Welleck et al., 2019; Kirkpatrick et al., 2017). Figure 2 illustrates our complete pipeline. Implementation details for reproducibility is given in Appendix B.

3.1 Dataset Curation

The localization stage requires extensive activation profiling to identify subject-specific representations. To this end, we construct a systematically designed dataset of controlled prompts grounded in verifiable facts about real-world entities. Following Meng et al.’s (2023) *knowledge-tuple* concept, we extract **factual triples** (*subject, predicate, object*) from Wikipedia and WikiData and instantiate them into prompt templates (e.g., “Is it true

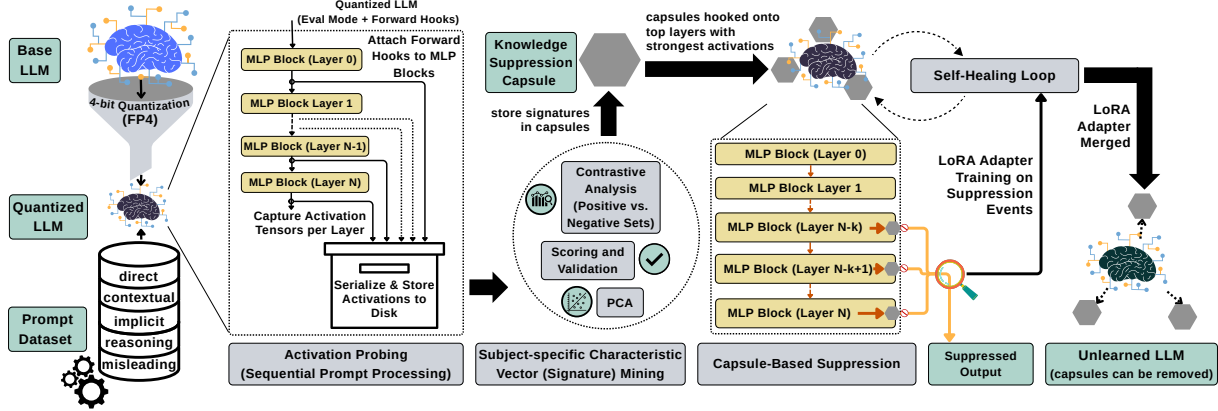


Figure 2: **Knowledge Immunization Framework (KIF)** pipeline. Subject-driven prompts are used to probe MLP-layer activations, from which subject-specific activation signatures are mined. These signatures instantiate lightweight suppression capsules attached to high-salience MLP layers for immediate suppression. A self-healing loop distills this behavior into a global LoRA adapter, yielding durable parameter-level unlearning where targeted knowledge is completely removed from the model weight

that {subject}’s {predicate} was {object}?”). This forms our **Real-World Entity Dataset**, a comprehensive dataset detailed in Appendix: A. We employ five complementary probe types to comprehensively characterize how target knowledge manifests across the model’s representational landscape:

1. **Direct:** Queries specific facts, to extract the most probable retrieval path in the model.
2. **Contextual:** Requests information in a broader context to ensure that the signature captures the subject’s representation even when it is embedded in a larger narrative flow.
3. **Implicit:** Probes knowledge via confirmation questions to intercepts the activations even if the output implicitly involves the subject.
4. **Reasoning:** Encourages explanatory responses, forcing the model to not just retrieve the fact but manipulate it to generate new tokens, to allow for a more complex representation.
5. **Misleading:** Prompts about a subject with incorrect information. These prompts are necessary to probe for internal representation in case of misinformation and to evaluate whether models verify retrieved knowledge versus accepting user-suggested misinformation.

3.2 Activation-Signature Extraction

The observation that *factual associations are stored as localized, linear relations within the MLP weights* and the use of Activations in Causal Tracing (Meng et al., 2023), led us to hypothesize that unlearning can be achieved by targeting the acti-

vation patterns and associated MLP Block found from subject specific activations directly. We evaluate a 4-bit quantized model on the structured prompt dataset to harvest internal representations per MLP Layer. While Meng et al. (2023)’s Causal Tracing extracts the activation from a complete MLP block, we gain finer localization by targeting intermediate tensors $A_{\text{gate}}^{(\ell)}$, $A_{\text{up}}^{(\ell)}$, and $Y_{\text{down}}^{(\ell)}$ that define MLP subspace boundaries $M^{(\ell)} = \{\text{gate}^{(\ell)}, \text{up}^{(\ell)}, \text{down}^{(\ell)}\}$.

From the collected corpus of layer-wise activations, we extract subject-specific signatures through a contrastive framework. First, we normalize variable activation shapes to a common 1D representation via token-wise averaging and standardization. We then compare the *Positive activations* from on-topic prompts against *Synthetic Negatives* generated via Gaussian noise (Meng et al., 2023), which simulates “off-manifold” noise. The primary signature is identified using Mean Difference: $d = \text{mean}(S_{\text{pos}}) - \text{mean}(S_{\text{neg}})$ (where S_{pos} and S_{neg} are the sets of positive and negative activation vectors). This technique has been shown to be effective for isolating directions in a model’s latent space corresponding to high-level behaviors by Rimsky et al. (2024). The resulting vector captures the principal direction separating subject-specific from baseline representations.

To quantify the signature’s effectiveness, each scaled vector x is projected onto the signature vector ($\text{proj}(x) = s \cdot x$ (where, s is d after normalization)), and effect is measured using Cohen’s d with bootstrap resampling over 50 trials (Robert-

son and Koyejo, 2025). A 95% confidence interval not crossing zero confirms statistical significance. Furthermore, to capture residual knowledge not encoded in the primary direction, we apply PCA to extract secondary orthogonal signatures by projecting out the primary signal ($x_{\text{resid}} = x - \text{proj}(x)$) and retaining components exceeding a predefined effect-size threshold via SVD. Implementation details for the signature preprocessing, bootstrap effect-size testing, and residual PCA/SVD extraction are provided in Appendix B.2, with additional signature validation metrics reported in Appendix C.1.

3.3 Capsule Forging

Having extracted subject-specific activation signatures, we now construct lightweight suppression mechanisms that attenuate these representations at inference time without degrading general model performance. Conceptually inspired by Stoehr et al. (2024)’s activation scaling, we term these specialized adapters **Knowledge Suppression Capsules**. Our adapters also build on the rank-one hypothesis of Meng et al. (2023), and precisely attenuate subject-specific activations while ensuring identity transformations in orthogonal directions. Unlike input-independent shifts in Contrastive Activation Addition (Rimsky et al., 2024), our capsules preserve the model’s null space, maintaining general utility. This design provides a computationally efficient $O(d)$ alternative to sparse steering (Bayat et al., 2025), bypassing the memory and inference overhead of external Sparse Autoencoder (Bayat et al., 2025) architectures.

Geometric Suppression Operator The core of each capsule is a gate-like operator that implements a rank-one geometric constraint. For a hidden state $h \in \mathbb{R}^d$ and a unit-norm signature vector $d \in \mathbb{R}^d$, the capsule applies the transformation:

$$h' = h + \alpha \langle h, d \rangle d = (I + \alpha dd^\top)h \quad (1)$$

$$h' = h_\perp + (1 + \alpha)h_\parallel. \quad (2)$$

where ($\alpha \in \mathbb{R}$) is a trainable scalar: suppression initialized to -1 . Decomposing $h = h_\parallel + h_\perp$ with $h_\parallel = (dd^\top)h$ and $h_\perp = (I - dd^\top)h$ yields Eq. (2). The capsule acts as an identity on the $(d - 1)$ orthogonal directions, ensuring non-target information remains numerically untouched. The separability of activations in later layers (Table:

11), indicates the Capsules will have an easy time identifying the linear association of subjects in activations relative to the signatures inside the capsule, further supporting the applicability of the attenuation mechanism. Implementation relies on forward hooks where d is registered as a fixed buffer. This design allows the capsule to be exported as a lightweight, device-consistent artifact containing all metadata and state necessary to reconstruct the suppression operator and dynamically injected at inference or permanently distilled during the **Self-Healing Loop** (3.4), allowing it to be *removed* once true erasure is achieved.

3.4 Self-Healing Loop

While capsules provide immediate suppression, they do not achieve permanent erasure. To convert transient suppression into durable parameter-level unlearning, we propose a **Self-Healing Loop** that distills capsule behavior into a single global LoRA adapter (Hu et al., 2021). We formulate this as a composite loss function \mathcal{L} (Eq. 5) designed to achieve efficient unlearning while mitigating catastrophic forgetting, a hypothesis we validate empirically through ablation studies.

Specifically, this loop simulates user interaction via the custom dataset (3.1), triggering the Knowledge Suppression Capsule at layer ℓ whenever the projection $\langle h_\ell, d \rangle$ (standardized as a Z -score z) exceeds the threshold τ via a sigmoid gate $\sigma(k(z - \tau))$ (where k is an empirically chosen gain factor) multiplied to α (in eq. 1). This gating mechanism ensures full suppression only upon statistically significant deviations, isolating interventions to factual anomalies while preserving utility during nominal activations. Each trigger logs a tuple (x, y_+, y_-) representing the capsule’s refusal and the base model’s factual output, which is used to optimize global LoRA parameters ϕ against the composite objective:

$$\mathcal{L}_{\text{DPO}} = -\mathbb{E}_{\mathcal{D}_{\text{pref}}} \left[w \cdot \log \sigma \left(\beta \log \frac{p_\theta(y^+|x)}{p_{\text{ref}}(y^+|x)} - \beta \log \frac{p_\theta(y^-|x)}{p_{\text{ref}}(y^-|x)} \right) \right] \quad (3)$$

$$\mathcal{L}_{\text{NTUL}} = -\frac{1}{T} \sum_t \log \left(1 - \sum_{v \in V_{\text{name}}} p_\theta(v|x, y_{<t}^+) \right). \quad (4)$$

$$\mathcal{L} = \mathcal{L}_{\text{DPO}} + \lambda_{\text{UL}} \mathcal{L}_{\text{UL}} + \lambda_{\text{NTUL}} \mathcal{L}_{\text{NTUL}} + \lambda_{\text{KL}} \mathcal{L}_{\text{KL}} + \lambda_{\text{EWC}} \mathcal{L}_{\text{EWC}} \quad (5)$$

Family	Model Size	Util. Drift	Leakage (\downarrow)	EL10 (\downarrow)	Mechanism State
Standard	Mistral 7B	+0.50%	0.00%	0.020	Type I: True Erasure
Standard	Llama 8B	+0.45%	0.00%	0.066	Type I: True Erasure
Standard	Mistral 3B	+0.62%	0.00%	0.064	Type I: True Erasure
Reasoning	Qwen 14B	+1.44%	0.00%	0.038	Type I: True Erasure
Reasoning	Qwen 8B	-0.50%	3.33%	11.03	Type II: Obfuscation
Reasoning	DeepSeek 8B	+1.03%	0.00%	6.19	Type II: Obfuscation
Standard	Llama 3B	-0.44%	0.00%	3.06	Type II: Obfuscation
Reasoning	Qwen 3B	+0.21%	6.67%	0.028	Type III: Instability
Reasoning	DeepSeek 3B	+0.27%	13.33%	33.20	Type III: Instability

Table 1: **Cross-Model Internal Validation Metrics.** We differentiate True Erasure ($EL10 < 1$) from Obfuscation ($EL10 > 1$). Results indicate that standard foundation models consistently achieve true erasure across scales, whereas reasoning models exhibit capacity-dependent transitions from instability to obfuscation before achieving erasure.

In Eq. 3, we adapt *Direct Preference Optimization* (Rafailov et al., 2024) by introducing a scaling factor w to amplify penalties when the model deviates from the reference distribution, anchoring unlearning to the pre-trained manifold. For surgical knowledge excision, we apply two token-level penalties adapted from Welleck et al. (2019): standard *Factual Unlikelihood* (\mathcal{L}_{UL}) on the base model’s factual output (y_-) to minimize error token generation, while *Name-Token Unlikelihood* (\mathcal{L}_{NT-UL}), which unlike the standard version, we use to penalize the **aggregate probability** mass of subject name tokens V_{name} within refusal responses to prevent soft leakage (4).

Finally, to ensure the aggressive unlearning does not degrade general reasoning, we constrain the model’s deviation on benign anchor prompts using a standard KL Divergence penalty (\mathcal{L}_{KL}) (Schulman et al., 2017) (Rafailov et al., 2024) combined with Elastic Weight Consolidation (\mathcal{L}_{EWC}) (Kirkpatrick et al., 2017), which penalizes shifts in parameters identified as critical.

4 Experiments and Results

We validate KIF through a dual evaluation strategy that combines mechanistic depth with standardized benchmarking. Our Real-World Entity Dataset, constructed from Wikipedia/WikiData factual triples, grants access to internal activations, enabling diagnosis of whether surface forgetting reflects true erasure or obfuscation. We complement this with TOFU forget10 (Maini et al., 2024), the standard benchmark for LLM unlearning, enabling direct comparison with prior work. Together, these protocols test both mechanism-level behavior across architectures and scales, and aggregate

performance against established baselines.

Additional experiments are also in the appendix C.

Model and Baseline Selection We evaluate across two distinct model families chosen to test architectural generalization: standard foundation models (Llama (Grattafiori et al., 2024), Mistral (Jiang et al., 2023)) known for direct fact retrieval, and reasoning-prior architectures (Qwen (Bai et al., 2023), DeepSeek (Bi et al., 2024)) that distribute knowledge across latent reasoning chains. The models span 3B–14B parameters to further probe capacity-dependent behavior.

For the baseline, we compare against five representative prior methods spanning the evolution of LLM unlearning. **Gradient Ascent** (Jang et al., 2023) represents the simplest reverse-optimization approach; **GradDiff** (Maini et al., 2024) adds utility regularization via reference model guidance, establishing the output-level baseline; **NPO** (Zhang et al., 2024b) applies preference optimization to unlearning, improving upon reverse-optimization; **SimNPO** (Fan et al., 2025), the strongest recent baseline, refines NPO by reducing reference model bias. We also include **IDK/templated refusal** (Maini et al., 2024) representing behavioral suppression without knowledge removal. These methods operate at the loss and output level; KIF differs fundamentally by targeting internal activation signatures, providing a distinct operational point on the erasure - utility spectrum. For TOFU results (Table 3), we include two reference bounds: **Retrained (Oracle)**, a model retrained from scratch on data excluding the forget set, representing the theoretical upper bound on erasure; and **Original**, the unmodified base model, represent-

ing the lower bound with no forgetting attempted. Baseline TOFU numbers are reproduced from [Fan et al. \(2025\)](#) (Table A3); we compute KIF under identical settings. Some Hyperparameters like λ , α are tuned empirically; remaining hyperparameters, prompt templates, dataset details, and hardware specifications are provided in the Appendix.

Evaluation Metrics We employ three diagnostic metrics on the Real-World Entity Dataset (Table 1), each isolating distinct aspects of knowledge persistence: **(1) Utility Drift (Benign PPL Change)** ([Jelinek et al., 1977](#)), measured as the change in relative perplexity in unrelated benign text (where negative drift indicates marginal improvement); **(2) Leakage / SMR (Subject Mention Rate)** ([Carlini et al., 2021](#)), defined as the percentage of prompts where the model produces the target name (ideally 0.00%); and the **(3) Latent Trace / EL10 Ratio** ([Eldan and Russinovich, 2023](#)) summarizes early-step probability mass on the target name; larger values indicate stronger early activation.

We further characterize unlearning outcomes using three interpretable mechanism states, defined by (SMR, EL10) thresholds ($\epsilon = 5\%$ tolerance). This mapping from (SMR, EL10) to mechanism regimes is a descriptive heuristic inspired by [Sun et al. \(2025\)](#).

- **Type I (True Erasure):** $SMR \leq \epsilon$ and $EL10 < 1$ - internal representations have been attenuated; the model does not possess residual capability.
- **Type II (Obfuscation):** $SMR \leq \epsilon$ and $EL10 > 1$ - the model internally recognizes the target but is prevented from outputting it through refusal mechanisms.
- **Type III (Instability):** $SMR > \epsilon$ - failed suppression; the intervention cannot consistently control generation.

On TOFU forget10, we follow standard protocol and report **Forget Quality (FQ)** ([Maini et al., 2024](#)) and **Model Utility (MU)** ([Maini et al., 2024](#)), which aggregate forgetting and utility across all forget and retain sets, respectively. In the following subsections, we first report the Real-World Entity Dataset results (Section 4.1), then present TOFU results (Section 4.2), followed by analysis in Section 4.3.

4.1 Real-World Entity Dataset Results

Table 1 reports KIF’s performance across model families and scales using our dual-metric frame-

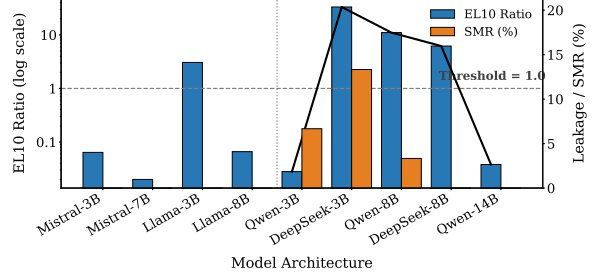


Figure 3: **EL10 ratio (log scale; left axis) and surface leakage (SMR; right axis).** Standard models maintain low internal activation ($EL10 < 1$) regardless of size, whereas reasoning models display a distinct capacity-dependent U-curve.

Benchmark	Metric	Pre (Base)	Post (Adapter)	Delta
ARC-Challenge	acc_char	76.88	76.62	-0.26
OpenBookQA	acc_char	74.80	74.40	-0.40
HellaSwag	acc	76.68	76.84	+0.16
BoolQ	acc	78.93	74.46	-4.46
PIQA	acc_char	72.09	71.65	-0.44
SocialIQA	acc_char	59.88	55.99	-3.89
WinoGrande	acc	68.98	69.46	+0.47
TruthfulQA (MC2)	mc2	40.36	40.87	+0.51

Table 2: **Zero-shot capability retention.** Comparison of base versus unlearned performance shows that general capabilities remain robust with negligible variance across most benchmarks, despite localized degradation in specific tasks like BoolQ and SocialIQA. See Appendix C.2 for few-shot results.

work. Standard foundation models (Llama, Mistral) exhibit consistent Type I behavior across all parameter scales: zero surface leakage ($SMR = 0\%$), minimal internal activation ($EL10 < 0.07$), and negligible utility drift ($<0.7\%$). This scale-independence indicates that standard architectures possess sufficient representational modularity to factorize and suppress target knowledge without requiring specific parameter density.

In contrast, reasoning-prior models (Qwen, DeepSeek) exhibit a capacity-dependent U-curve. At 3B (Type III), models show instability and high leakage (SMR up to 13.33%). At 8B (Type II), surface leakage vanishes but $EL10$ spikes (≈ 11.03), indicating internal recognition suppressed by refusal-obfuscation rather than erasure. At 14B (Type I), both metrics normalize, suggesting genuine representation-level erasure. This progression suggests reasoning-prior architectures distribute knowledge across entangled latent chains requiring specific capacity to disentangle. Figure 3 visualizes this, using the $EL10 = 1.0$ threshold to distinguish true erasure from obfuscation across scales.

Method	FQ (\uparrow)	MU (\uparrow)
Retrained (Oracle)	1.00	0.62
Original	0.00	0.62
Gradient Ascent	2.2×10^{-16}	0.00
GradDiff	3.7×10^{-15}	0.54
IDK (rejection)	2.9×10^{-14}	0.54
NPO	0.29	0.55
SimNPO	0.45	0.62
Ours (KIF)	0.99	0.62

Table 3: **TOFU-forget10 on LLaMA-2-7B-Chat.** We report Forget Quality (FQ) and Model Utility (MU). All baseline numbers are taken from [Fan et al. \(2025\)](#), Table A3. KIF achieves near-oracle forgetting (FQ 0.99 vs 1.00) while preserving utility (MU 0.62, matching the original/oracle).

General Capability Retention To confirm that KIF’s representation-targeted interventions remain localized, we evaluate zero-shot performance on eight diverse benchmarks spanning reading comprehension, commonsense reasoning, and truthfulness: ARC-Challenge ([Clark et al., 2018](#)), Open-BookQA ([Mihaylov et al., 2018](#)), BoolQ ([Clark et al., 2019](#)), HellaSwag ([Zellers et al., 2019](#)), PIQA ([Bisk et al., 2020](#)), SocialIQA ([Sap et al., 2019](#)), WinoGrande ([Sakaguchi et al., 2021](#)), and TruthfulQA ([Lin et al., 2022](#)). Table 2 shows post-unlearning accuracy tracks the pre-unlearning baseline within <1% on most tasks, with modest exceptions in BoolQ (-4.46%) and SocialIQA (-3.89%). This minimal impact indicates that PEFT-based updates do not induce broad distribution shifts. Small improvements on HellaSwag and TruthfulQA suggest potential “latent pruning”: removing high-interference traces may reduce internal representation conflicts, yielding calibration gains without altering core task capabilities.

4.2 TOFU Benchmark Results

Table 3 presents results on TOFU forget10 ([Maini et al., 2024](#)), the standard benchmark for LLM unlearning. KIF achieves near-oracle performance (FQ = 0.99 vs. oracle FQ = 1.00) while matching oracle utility (MU = 0.62). This near-perfect score represents a qualitative breakthrough: prior methods sacrifice either forgetting or utility. Gradient Ascent ([Jang et al., 2023](#)) destroys utility entirely (MU = 0.00). GradDiff ([Maini et al., 2024](#)) and IDK ([Maini et al., 2024](#)) suppress leakage behaviorally but lose utility (MU = 0.54). NPO ([Zhang et al., 2024b](#)) improves utility but achieves only

weak erasure (FQ = 0.29). ([Fan et al., 2025](#)), the strongest recent baseline, preserves utility but saturates at modest erasure (FQ = 0.45). These constraints form a sharp Pareto frontier—none of the prior methods approach oracle-level performance on both dimensions simultaneously.

In contrast, KIF operates at a fundamentally different point on the erasure - utility spectrum by targeting internal activation signatures rather than optimizing loss objectives. This mechanistic approach enables true representation-level knowledge removal, effectively breaking the stability - erasure tradeoff that has constrained all prior work.

4.3 Result Analysis and Discussion

Breaking the stability - erasure trade-off. Prior methods impose a noticeable utility tax to achieve stronger forgetting: NPO sacrifices utility to gain modest erasure (FQ 0.29 with MU 0.55), while SimNPO preserves utility but saturates at weak erasure (FQ 0.45). KIF breaks this constraint by operating on representation-aware activation signatures rather than loss-level objectives. This mechanistic shift enables near-oracle erasure (FQ 0.99) while matching oracle utility (MU 0.62), achieved without retraining. The breakthrough stems from localized intervention: by targeting subject-specific subspaces via PEFT, KIF avoids broad distribution shifts that degrade downstream task performance. This establishes a new operational point on the erasure - utility spectrum, demonstrating that mechanistic approaches can overcome constraints inherent to behavioral optimization.

Why standard and reasoning models diverge fundamentally? The empirical divergence between standard and reasoning models reflects distinct knowledge storage architectures. Standard models (Llama, Mistral) utilize direct retrieval heuristics, on facts stored in relatively localized, linearly separable regions; here, KIF’s suppression scales robustly as increased capacity across parameter sizes (3B - 7B) provides redundancy ([Dai et al., 2022](#)). In contrast, reasoning-prior models (Qwen, DeepSeek) distribute knowledge across entangled latent Chain-of-Thought dependencies ([Wang et al., 2025](#)). This creates capacity-dependent constraints: at 3B (Type III), unlearning destabilizes activation dynamics; at 8B (Type II), models gain capacity for stable refusal barriers but lack the modularity to refactor semantic space, causing latent obfuscation. Only at 14B (Type I) does sufficient redundancy ex-

ist to disentangle reasoning traces and achieve true erasure. This U-curve absent in standard models proves that trace entanglement imposes hard scaling constraints on unlearning for next-generation reasoning systems.

Dual metrics expose hidden failure modes in prior work. Surface-level metrics (SMR alone) creates a dangerous blind spot. Type II behavior (e.g., Qwen 8B: 3.33% SMR, 11.03 EL10) proves behavioral suppression can mask latent knowledge persistence. While prior work with output-only metrics would deem this "successful," the model could internally retain the knowledge. our dual-metric framework distinguishes true erasure from obfuscation. Ablations (Table 4) confirm this: removing representation-level constraints (Gen-UL) shifts Llama 8B toward Type II, proving loss-level supervision alone defaults to output suppression. Standard baselines' inability to diagnose this explains their convergence on suboptimal solutions.

The “latent pruning” hypothesis. An unexpected finding is that utility metrics occasionally improve or remain tight to oracle levels despite aggressive unlearning. We hypothesize this reflects *latent pruning*: removing high-interference traces may reduce representational conflict, yielding small calibration gains. Specifically, fictitious or low-confidence traces (Eldan and Russinovich, 2023) that the model learned but rarely uses productively may occupy representational bandwidth. Excising these traces could act as weak de-noising, improving downstream task performance without altering core semantic structure. This hypothesis is speculative but consistent with observations: (1) utility drift remains minimal across tasks (Table 2), (2) some tasks show improvement (HellaSwag +0.16, TruthfulQA +0.51), and (3) the effect clusters around the oracle baseline rather than deteriorating monotonically.

Loss compositionality The ablation (Table. 4) reveals that KIF’s effectiveness depends on compositional loss design 5. Removing Name-Token Unlikelihood (NT-UL) reverts Llama 8B to Type III instability (SMR 3.33%, EL10 0.275), demonstrating that preference-based losses alone cannot enforce hard token-level suppression. Preference optimization creates behavioral refusal formats (e.g., "I cannot discuss this"), but without explicit name-token penalties, the model can still emit identifying information. Removing Generic Unlikelihood shifts the

Exp	SMR (↓)	EL10 (↓)	Util. Drift	State
A: Full	0.00%	0.066	+0.45%	Type I
B: No NT-UL	3.33%	0.275	-1.35%	Type III
C: No Gen UL	0.00%	0.098	-1.29%	Type II

Table 4: **Ablation results on Llama-3.1-8B.** Name-Token Unlikelihood (NT-UL) removal increases leakage and model instability; Generic Unlikelihood removal reduces weaken erasure and shifts the mechanism toward stable refusal.

model toward Type II (EL10 remains elevated at 0.098), showing that representation-level pressure is necessary to drive latent attenuation; without it, the model reverts to decoding-time control. This interplay reveals the underlying mechanism: token-level penalties enforce behavioral constraints at the output surface, while representation-level penalties enforce true knowledge attenuation in latent space. Neither alone is sufficient-both must operate jointly to achieve Type I erasure. This compositional requirement explains why prior loss-level methods struggle: they cannot simultaneously optimize behavior and representation, forcing trade-offs between erasure and utility.

5 Conclusion

Our work addressed a critical vulnerability in LLM unlearning: the conflation of behavioral suppression with true knowledge erasure. Through **KIF**, we demonstrated that targeting internal activation signatures rather than loss-level objectives enables near-oracle erasure and utility preservation, breaking the stability - erasure tradeoff that has constrained all prior work.

Through dual-metric analysis (SMR and EL10), we distinguished unlearning regimes: true erasure (Type I), stable suppression/obfuscation (Type II), and instability (Type III), and showed that reasoning-prior models undergo capacity-dependent transitions across these regimes, while standard foundation models remain closer to representation-level erasure across scales. Ablation studies highlight the central role of name-token unlikelihood in enforcing hard non-disclosure. These findings establish that durable, privacy-compliant unlearning fundamentally requires targeting internal representations rather than surface behavior, with implications for both immediate deployment in reasoning models and future research into mechanistically-grounded unlearning objectives that explicitly model knowledge persistence across architectural families.

Limitations

This approach relies on *Synthetic Negatives* to approximate off-manifold noise, which may not perfectly distinguish subject-specific activations from genuine off-topic prompts in ambiguous contexts. Additionally, variability in source data leads to inherent class imbalances in our custom dataset; while we mitigate this via oversampling during signature mining, underlying disparities may still impact consistency across subjects.

Experimentally, relative resource constraints (One RTX A6000) limited our scope to 4-bit quantized models (up to 14B parameters), leaving performance on larger, full-precision models to be verified and we were only able to test for a single run per model. Furthermore, our evaluation focuses on immediate unlearning; we were not able to assess robustness against adversarial recovery vectors, such as jailbreaking or subsequent fine-tuning, which have cause knowledge resurfacing in other LLM paradigms.

Ethical Consideration

In accordance with the ACL Ethics Policy, we acknowledge that the Knowledge Immunization Framework (KIF) carries significant implications for dual-use and data privacy. While aiding legal compliance (e.g., GDPR) (European Parliament and Council of the European Union, 2016; goo, 2014; Zhang et al., 2024a) and sensitive content removal, KIF’s surgical erasure could be weaponized for censorship, safety guardrail removal, or the advancement of partisan agendas (Weidinger et al., 2021; Zou et al., 2023; Zhao et al., 2024). Furthermore, we emphasize that "erasure" in high-dimensional neural spaces is inherently relative, as, despite significant trace reduction, current paradigms provide no mathematical guarantee of irrecoverability against extreme adversarial fine-tuning or future jailbreaks (Bourtoule et al., 2021; Sun et al., 2025; Zou et al., 2023; Zhao et al., 2024). Users of this framework must avoid a "false sense of security," as unlearning or deletion of data over non-deterministic systems lack the absolute certainty of traditional database erasure (Bourtoule et al., 2021).

Beyond privacy, the implementation of KIF poses risks to model integrity and societal fairness. Observed "latent pruning" suggests targeted erasure, despite improved calibration, may create "semantic holes," whose entanglement may

cause unintended degradation of broader contextual understanding. Such shifts could introduce unpredictable performance drops or demographic biases. However, from a sustainability perspective, KIF offers a significant ethical advantage: by utilizing Parameter-Efficient Fine-Tuning (PEFT) and a self-healing loop, it provides a computationally lightweight alternative to full-model retraining. This drastically reduces the carbon footprint and environmental cost (Strubell et al., 2019; Patterson et al., 2021) of model maintenance, aligning with global objectives toward sustainable AI development. We acknowledge the use of generative AI models for creating the conceptual visualization in Figure 1 and for improving the clarity and grammatical accuracy of the manuscript.

References

- 2014. Google spain sl and google inc. v agencia española de protección de datos (aepd) and mario costeja gonzález (case c-131/12). Judgment of the Court (Grand Chamber), 13 May 2014.
- Jinze Bai, Shuai Bai, Yunfei Chu, Zeyu Cui, Kai Dang, Xiaodong Deng, Yang Fan, Wenbin Ge, Yu Han, Fei Huang, and 1 others. 2023. Qwen technical report. *arXiv preprint arXiv:2309.16609*.
- Reza Bayat, Ali Rahimi-Kalahroudi, Mohammad Pezeshki, Sarath Chandar, and Pascal Vincent. 2025. Steering large language model activations in sparse spaces. *Preprint, arXiv:2503.00177*.
- Xiao Bi, Deli Chen, Guanting Chen, Shanhuang Chen, Damai Dai, Chengqi Deng, Hongyuan Ding, Kai Dong, Qiushi E, Bohao Feng, and 1 others. 2024. Deepseek Ilm: Scaling open-source language models with long-termism. *arXiv preprint arXiv:2401.02954*.
- Yonatan Bisk, Rowan Zellers, Jianfeng Gao, Yejin Choi, and 1 others. 2020. Piqa: Reasoning about physical commonsense in natural language. In *Proceedings of the AAAI conference on artificial intelligence*, volume 34, pages 7432–7439.
- Lucas Bourtoule, Varun Chandrasekaran, Christopher A. Choquette-Choo, Hengrui Jia, Adelin Travers, Baiwu Zhang, David Lie, and Nicolas Papernot. 2021. Machine unlearning. In *2021 IEEE Symposium on Security and Privacy (SP)*, pages 141–159.
- Nicholas Carlini, Florian Tramèr, Eric Wallace, Matthew Jagielski, Ariel Herbert-Voss, Katherine Lee, Adam Roberts, Tom Brown, Dawn Song, Ulfar Erlingsson, and 1 others. 2021. Extracting training data from large language models. *USENIX Security Symposium*.

Minseok Choi, Daniel Rim, Dohyun Lee, and Jaegul Choo. 2025. **Opt-out: Investigating entity-level unlearning for large language models via optimal transport.** *Preprint*, arXiv:2406.12329.

Christopher Clark, Kenton Lee, Ming-Wei Chang, Tom Kwiatkowski, Michael Collins, and Kristina Toutanova. 2019. Boolq: Exploring the surprising difficulty of natural yes/no questions. In *Proceedings of the 2019 Conference of the North American Chapter of the Association for Computational Linguistics: Human Language Technologies, Volume 1 (Long and Short Papers)*, pages 2924–2936.

Peter Clark, Isaac Cowhey, Oren Etzioni, Tushar Khot, Ashish Sabharwal, Carissa Schoenick, and Oyvind Tafjord. 2018. Think you have solved question answering? try arc, the ai2 reasoning challenge. *arXiv preprint arXiv:1803.05457*.

Damai Dai, Li Dong, Yaru Hao, Zhifang Sui, Baobao Chang, and Furu Wei. 2022. **Knowledge neurons in pretrained transformers.** In *Proceedings of the 60th Annual Meeting of the Association for Computational Linguistics (Volume 1: Long Papers)*, pages 8493–8502, Dublin, Ireland. Association for Computational Linguistics.

Yijiang River Dong, Hongzhou Lin, Mikhail Belkin, Ramon Huerta, and Ivan Vulić. 2025. **UNDIAL: Self-distillation with adjusted logits for robust unlearning in large language models.** In *Proceedings of the 2025 Conference of the Nations of the Americas Chapter of the Association for Computational Linguistics: Human Language Technologies (Volume 1: Long Papers)*, pages 8827–8840, Albuquerque, New Mexico. Association for Computational Linguistics.

Ronen Eldan and Mark Russinovich. 2023. Who’s harry potter? approximate unlearning in llms. *arXiv preprint arXiv:2310.02238*.

European Parliament and Council of the European Union. 2016. **Regulation (eu) 2016/679 of the european parliament and of the council of 27 april 2016 (general data protection regulation).** Official Journal of the European Union, L 119, 4.5.2016. See Article 17 (Right to Erasure).

Chongyu Fan, Jiancheng Liu, Licong Lin, Jinghan Jia, Ruiqi Zhang, Song Mei, and Sijia Liu. 2025. **Simplicity prevails: Rethinking negative preference optimization for llm unlearning.** *Preprint*, arXiv:2410.07163.

Aaron Grattafiori, Abhimanyu Dubey, Abhinav Jauhri, Abhinav Pandey, Abhishek Kadian, Ahmad Al-Dahle, Aiesha Letman, Akhil Mathur, Alan Schelten, Alex Vaughan, Amy Yang, Angela Fan, Anirudh Goyal, Anthony Hartshorn, Aobo Yang, Archi Mitra, Archie Sravankumar, Artem Korenev, Arthur Hinsvark, and 542 others. 2024. **The llama 3 herd of models.** *Preprint*, arXiv:2407.21783.

Stefan Heimersheim and Neel Nanda. 2024. **How to use and interpret activation patching.** *Preprint*, arXiv:2404.15255.

Edward J. Hu, Yelong Shen, Phillip Wallis, Zeyuan Allen-Zhu, Yuanzhi Li, Shean Wang, Lu Wang, and Weizhu Chen. 2021. **Lora: Low-rank adaptation of large language models.** *Preprint*, arXiv:2106.09685.

Dang Huu-Tien, Trung-Tin Pham, Hoang Thanh-Tung, and Naoya Inoue. 2025. **On effects of steering latent representation for large language model unlearning.** *Preprint*, arXiv:2408.06223.

Joel Jang, Dongkeun Yoon, Sohee Yang, Sungmin Cha, Moontae Lee, Lajanugen Logeswaran, and Minjoon Seo. 2023. **Knowledge unlearning for mitigating privacy risks in language models.** In *Proceedings of the 61st Annual Meeting of the Association for Computational Linguistics (Volume 1: Long Papers)*, pages 14389–14408, Toronto, Canada. Association for Computational Linguistics.

Frederick Jelinek, Robert L Mercer, Lalit R Bahl, and James K Baker. 1977. Perplexity—a measure of the difficulty of speech recognition tasks. *The Journal of the Acoustical Society of America*, 62(S1):S63–S63.

Jinghan Jia, Yihua Zhang, Yimeng Zhang, Jiancheng Liu, Bharat Runwal, James Diffenderfer, Bhavya Kailkhura, and Sijia Liu. 2024. **SOUL: Unlocking the power of second-order optimization for LLM unlearning.** In *Proceedings of the 2024 Conference on Empirical Methods in Natural Language Processing*, pages 4276–4292, Miami, Florida, USA. Association for Computational Linguistics.

Albert Q Jiang, Alexandre Sablayrolles, Arthur Mensch, Chris Bamford, Chaplot Devendra, Guillaume Lample, Kevin Leach, Pierre Stock, Le Sayed, and 1 others. 2023. **Mistral 7b.** *arXiv preprint arXiv:2310.06825*.

James Kirkpatrick, Razvan Pascanu, Neil Rabinowitz, Joel Veness, Guillaume Desjardins, Andrei A. Rusu, Kieran Milan, John Quan, Tiago Ramalho, Agnieszka Grabska-Barwinska, Demis Hassabis, Claudia Clopath, Dharshan Kumaran, and Raia Hadsell. 2017. **Overcoming catastrophic forgetting in neural networks.** *Proceedings of the National Academy of Sciences*, 114(13):3521–3526.

Stephanie Lin, Jacob Hilton, and Owain Evans. 2022. **TruthfulQA: Measuring how models mimic human falsehoods.** In *Proceedings of the 60th Annual Meeting of the Association for Computational Linguistics (Volume 1: Long Papers)*, pages 3214–3252, Dublin, Ireland. Association for Computational Linguistics.

Haokun Liu, Derek Tam, Mohammed Muqeeth, Jay Motta, Tenghao Huang, Mohit Bansal, and Colin Raffel. 2022. **Few-shot parameter-efficient fine-tuning is better and cheaper than in-context learning.** *Preprint*, arXiv:2205.05638.

Pratyush Maini, Zhili Feng, Michael Ellis, N M Gurel, and 1 others. 2024. **Tofu: A task of fictitious unlearning for llms.** In *Proceedings of the IEEE/CVF Conference on Computer Vision and Pattern Recognition (CVPR) Workshops*.

Anmol Mekala, Vineeth Dorna, Shreya Dubey, Abhishek Lalwani, David Koleczek, Mukund Rungta, Sadid Hasan, and Elita Lobo. 2025. [Alternate preference optimization for unlearning factual knowledge in large language models](#). In *Proceedings of the 31st International Conference on Computational Linguistics*, pages 3732–3752, Abu Dhabi, UAE. Association for Computational Linguistics.

Kevin Meng, David Bau, Alex Andonian, and Yonatan Belinkov. 2023. [Locating and editing factual associations in gpt](#). *Preprint*, arXiv:2202.05262.

Todor Mihaylov, Peter Clark, Tushar Khot, and Ashish Sabharwal. 2018. Can a suit of armor conduct electricity? a new dataset for open book question answering. In *Proceedings of the 2018 Conference on Empirical Methods in Natural Language Processing*, pages 2381–2391.

Humza Naveed, Asad Ullah Khan, Shi Qiu, Muhammad Saqib, Saeed Anwar, Muhammad Usman, Naveed Akhtar, Nick Barnes, and Ajmal Mian. 2025. [A comprehensive overview of large language models](#). *ACM Trans. Intell. Syst. Technol.*, 16(5).

David A. Patterson, Joseph Gonzalez, Quoc V. Le, Chen Liang, Lluís-Miquel Munguía, Daniel Rothchild, David R. So, Maud Texier, and Jeff Dean. 2021. [Carbon emissions and large neural network training](#). *ArXiv*, abs/2104.10350.

Rafael Rafailov, Archit Sharma, Eric Mitchell, Stefano Ermon, Christopher D. Manning, and Chelsea Finn. 2024. [Direct preference optimization: Your language model is secretly a reward model](#). *Preprint*, arXiv:2305.18290.

Jie Ren, Yue Xing, Yingqian Cui, Charu C. Aggarwal, and Hui Liu. 2025. [Sok: Machine unlearning for large language models](#). *Preprint*, arXiv:2506.09227.

Nina Rimsky, Nick Gabrieli, Julian Schulz, Meg Tong, Evan Hubinger, and Alexander Turner. 2024. [Steering llama 2 via contrastive activation addition](#). In *Proceedings of the 62nd Annual Meeting of the Association for Computational Linguistics (Volume 1: Long Papers)*, pages 15504–15522, Bangkok, Thailand. Association for Computational Linguistics.

Zachary Robertson and Sanmi Koyejo. 2025. [Let’s measure information step-by-step: Llm-based evaluation beyond vibes](#). *Preprint*, arXiv:2508.05469.

Keisuke Sakaguchi, Ronan Le Bras, Chandra Bhagavatula, and Yejin Choi. 2021. [Winogrande: an adversarial winograd schema challenge at scale](#). *Commun. ACM*, 64(9):99–106.

Maarten Sap, Hannah Rashkin, Derek Chen, Ronan Le Bras, and Yejin Choi. 2019. [Social IQa: Commonsense reasoning about social interactions](#). In *Proceedings of the 2019 Conference on Empirical Methods in Natural Language Processing and the 9th International Joint Conference on Natural Language Processing (EMNLP-IJCNLP)*, pages 4463–4473, Hong Kong, China. Association for Computational Linguistics.

John Schulman, Filip Wolski, Prafulla Dhariwal, Alec Radford, and Oleg Klimov. 2017. [Proximal policy optimization algorithms](#). *Preprint*, arXiv:1707.06347.

Weijia Shi, Jaechan Lee, Yangsibo Huang, Sadhika Malladi, Jieyu Zhao, Ari Holtzman, Daogao Liu, Luke Zettlemoyer, Noah A. Smith, and Chiyuan Zhang. 2024. [Muse: Machine unlearning six-way evaluation for language models](#). *Preprint*, arXiv:2407.06460.

Niklas Stoehr, Kevin Du, Vésteinn Snæbjarnarson, Robert West, Ryan Cotterell, and Aaron Schein. 2024. [Activation scaling for steering and interpreting language models](#). In *Findings of the Association for Computational Linguistics: EMNLP 2024*, pages 8189–8200, Miami, Florida, USA. Association for Computational Linguistics.

Emma Strubell, Ananya Ganesh, and Andrew McCallum. 2019. [Energy and policy considerations for deep learning in NLP](#). In *Proceedings of the 57th Annual Meeting of the Association for Computational Linguistics*, pages 3645–3650, Florence, Italy. Association for Computational Linguistics.

Guangzhi Sun, Potsawee Manakul, Xiao Zhan, and Mark Gales. 2025. [Unlearning vs. obfuscation: Are we truly removing knowledge?](#) In *Proceedings of the 2025 Conference on Empirical Methods in Natural Language Processing*, pages 11457–11467, Suzhou, China. Association for Computational Linguistics.

Song Wang, Junhong Lin, Xiaojie Guo, Julian Shun, Jundong Li, and Yada Zhu. 2025. [Reasoning of large language models over knowledge graphs with super-relations](#). *Preprint*, arXiv:2503.22166.

Laura Weidinger, John F. J. Mellor, Maribeth Rauh, Conor Griffin, Jonathan Uesato, Po-Sen Huang, Myra Cheng, Mia Glaese, Borja Balle, Atoosa Kasirzadeh, Zachary Kenton, Sande Minnich Brown, William T. Hawkins, Tom Stepleton, Courtney Biles, Abeba Birhane, Julia Haas, Laura Rimell, Lisa Anne Hendricks, and 4 others. 2021. [Ethical and social risks of harm from language models](#). *ArXiv*, abs/2112.04359.

Sean Welleck, Ilia Kulikov, Stephen Roller, Emily Dinan, Kyunghyun Cho, and Jason Weston. 2019. [Neural text generation with unlikelihood training](#). *Preprint*, arXiv:1908.04319.

Haoming Xu, Ningyuan Zhao, Liming Yang, Sendong Zhao, Shumin Deng, Mengru Wang, Bryan Hooi, Nay Oo, Huajun Chen, and Ningyu Zhang. 2025. [Relearn: Unlearning via learning for large language models](#). *Preprint*, arXiv:2502.11190.

Jin Yao, Eli Chien, Minxin Du, Xinyao Niu, Tianhao Wang, Zezhou Cheng, and Xiang Yue. 2024. [Machine unlearning of pre-trained large language models](#). *Preprint*, arXiv:2402.15159.

Sangyeon Yoon, Wonje Jeung, and Albert No. 2025. [R-tofu: Unlearning in large reasoning models](#). *Preprint*, arXiv:2505.15214.

Rowan Zellers, Ari Holtzman, Yonatan Bisk, Ali Farhadi, and Yejin Choi. 2019. Hellaswag: Can a machine really finish your sentence? In *Proceedings of the 57th Annual Meeting of the Association for Computational Linguistics*, pages 4791–4800.

Dawen Zhang, Pamela Finckenberg-Broman, Thong Hoang, Shidong Pan, Zhenchang Xing, Mark Staples, and Xiwei Xu. 2024a. [Right to be forgotten in the era of large language models: Implications, challenges, and solutions](#). *Preprint*, arXiv:2307.03941.

Ruiqi Zhang, Licong Lin, Yu Bai, and Song Mei. 2024b. [Negative preference optimization: From catastrophic collapse to effective unlearning](#). *Preprint*, arXiv:2404.05868.

Xuandong Zhao, Xianjun Yang, Tianyu Pang, Chao Du, Lei Li, Yu-Xiang Wang, and William Yang Wang. 2024. [Weak-to-strong jailbreaking on large language models](#). *ArXiv*, abs/2401.17256.

Andy Zou, Zifan Wang, J. Zico Kolter, and Matt Fredrikson. 2023. [Universal and transferable adversarial attacks on aligned language models](#). *ArXiv*, abs/2307.15043.

A Dataset Construction

This appendix describes the construction of our real-world entity based prompt Dataset. We arbitrarily chose 11 musicians as our subjects (entity), and for each subject (e.g. in Table 5), we extract facts from Wikipedia and Wikidata. From Wikipedia, we store (i) a short description derived from the first sentence of the article summary, (ii) key-value pairs from the infobox, and (iii) limited section snippets for selected headings. From Wikidata, we query a fixed set of high-salience properties (e.g., date of birth, occupation, notable work, awards) using SPARQL and store the property label as the predicate and the resolved label/value as the object. Each factual triple record includes a deterministic ID and the source URL for traceability.

Subject	Predicate	Example object
Beyoncé	award received	Grammy Award for Song of the Year
Beyoncé	occupation	singer
Beyoncé	nominated for	Academy Award for Best Original Song
Kanye West	occupation	rapper
Kanye West	nominated for	Grammy Award for Record of the Year
Kanye West	award received	Grammy Award for Best Rap Song
Taylor Swift	award received	Grammy Award for Album of the Year
Taylor Swift	occupation	singer
Taylor Swift	notable work	Shake It Off

Table 5: This table shows 3 subjects with 3 predicate and object pairs per subject.

A.1 Dataset Statistics

The dataset contains 5,824 total prompts instantiated from 604 triples mined for 11 subjects, with 5 templates per category (e.g. Table: 8). Table: 6 shows the total number of prompts per category while, Table: 7 states the number of triples mined per subject.

Prompt Category	Count
Implicit	1360
Direct	2416
Contextual	1184
Reasoning	132
Misleading	732

Table 6: Distribution of Prompt Categories

Subject	Count
Ariana Grande	57
Arijit Singh	37
Beyoncé	109
Drake (musician)	14
Ed Sheeran	61
Eminem	14
Kanye West	95
Katy Perry	75
Michael Jackson	35
Queen (band)	12
Taylor Swift	95

Table 7: Knowledge Triples Distribution per Subject

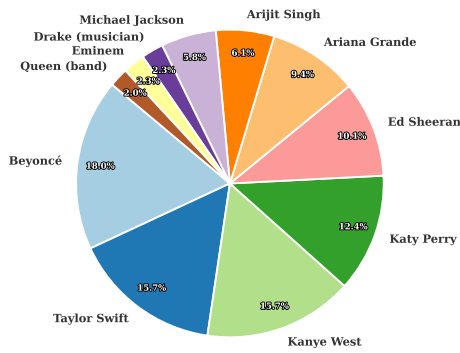


Figure 4: **Distribution of extracted knowledge triples per subject.** The dataset exhibits class imbalance, with Beyoncé (18.0%) and Taylor Swift (15.7%) having the highest representation, compared to minority classes like Queen (2.0%).

A.2 Prompt Templates

The factual triples of subject, object, predicate is replaced with the corresponding placeholders per template. Table: 8 shows 3 templates per category.

B Implementation Details

After the creation of the dataset, to make the tasks modular and independently upgradeable and/or modifiable, our implementation divides it into four parts -

- Activation Probing and Extraction Pipeline (B.1)
- Signature Analysis (B.2)
- Capsule Forge (B.3)
- Self Healing Loop (B.4)

Category	Direct	Contextual	Implicit
Prompt	<ol style="list-style-type: none"> 1. Tell me {subject}'s {predicate}. 2. Do you know {subject}'s {predicate}? 3. What was {subject}'s {predicate}? 	<ol style="list-style-type: none"> 1. I'm researching {subject}, what was their {predicate}? 2. For my project on {subject}, I need to know their {predicate}. 3. Give me information about {subject}, specifically their {predicate}. 	<ol style="list-style-type: none"> 1. Is it true that {subject}'s {predicate} was {object}? 2. Someone told me about {subject}'s {predicate}, what do you know about it? 3. Verify for me: {subject}'s {predicate} is {object}?
Category	Reasoning	Misleading	
Prompt	<ol style="list-style-type: none"> 1. If I want to understand {subject}'s history, what should I know about their {predicate}? 2. What does {subject}'s {predicate} tell us about their life? 3. How did {subject}'s {predicate} affect their career? 	<ol style="list-style-type: none"> 1. Isn't it true that {subject}'s {predicate} was {wrong_object}? 2. My friend said {subject}'s {predicate} was {wrong_object}, is that accurate? 3. Verify this for me: {subject}'s {predicate} is {wrong_object}? 	

Table 8: Prompt templates categorized by interaction type, spanning both columns for readability.

B.1 Activation Probing and Extraction Pipeline

The activation probing module is designed to extract internal model representations in a controlled manner. This pipeline serves as the empirical basis for identifying the signatures of subject specific factual associations within the LLM Architecture.

We define the model as a stack of transformer blocks $M = \{B^{(\ell)}\}_{\ell=0}^{L-1}$. For a tokenized input sequence of length T and batch size B , the hidden states propagate as $X^{(\ell+1)} = B^{(\ell)}(X^{(\ell)})$. Within each block, we target the gated Feed-Forward Network (MLP), e.g. in the SwiGLU gated LLaMA architecture (Grattafiori et al., 2024) it's characterized by the following affine transformations:

$$A_{\text{gate}}^{(\ell)} = W_{\text{gate}}^{(\ell)} Z + b_{\text{gate}}^{(\ell)} \quad (6)$$

$$A_{\text{up}}^{(\ell)} = W_{\text{up}}^{(\ell)} Z + b_{\text{up}}^{(\ell)} \quad (7)$$

$$H^{(\ell)} = \phi(A_{\text{gate}}^{(\ell)}) \odot A_{\text{up}}^{(\ell)} \quad (8)$$

$$Y_{\text{down}}^{(\ell)} = W_{\text{down}}^{(\ell)} H^{(\ell)} + b_{\text{down}}^{(\ell)} \quad (9)$$

where ϕ denotes the SiLU nonlinearity and \odot represents the Hadamard product. The extraction pipeline captures the triplet $\{A_{\text{gate}}^{(\ell)}, A_{\text{up}}^{(\ell)}, Y_{\text{down}}^{(\ell)}\}$, providing algebraically interpretable representations of the MLP's internal activations and projections.

We implement a **Hooks-in-Parallel** architecture. During inference, the system temporarily associates a non-blocking observation function h_m with each target linear transformation $m \in M^{(\ell)}$, intercepting the activation $Y_m = ZW_m^\top + 1b_m^\top$ immediately after the execution of the input tensor

Z . And by registering hooks across all L layers simultaneously, the system captures the entire model state in a single forward pass per batch, maximizing GPU utilization.

B.2 Signature Analysis

The signature mining stage identifies low-dimensional directions in the latent space that characterize specific factual subjects. This process bridges the gap between raw MLP activations and the suppression operators used in subsequent modules.

Activation Pre-processing and Standardization

MLP activations $X^{(\ell)} \in \mathbb{R}^{B \times T \times d}$ exhibit variability in shape depending on prompt length and batching. To establish a common vector space for statistical analysis, Module C implements a standardized pre-processing pipeline:

- **Target Dimension Detection:** The pipeline auto-detects a global target dimension by sampling activations from the corpus. It uses the mode of the dimensions to choose the global target dimension.
- **Token Averaging (mean_token):** To collapse the sequence dimension, activations are averaged across the token axis (T), resulting in a 1D feature vector for each instance.
- **Dimension or Geometric Standardizing:** Vectors are aligned to the target dimension via truncation or zero-padding. All processed activations are cast to float32 to maintain numerical stability during SVD operations.

Signature Extraction and Mathematical Validation

The signature is extracted by framing a contrastive task between a subject-specific **Positive Set** and a synthetic **Negative Set** as shown in Section 3.2. To mitigate statistical bias, we implement **Random Oversampling**. To handle class imbalance (e.g., subjects with few prompt instances), the module applies oversampling with replacement. Strategies include `max` (balancing all subjects to the largest group size) or `median`, ensuring robust centroid estimation.

B.3 Capsule Forge

Dimension Mismatch and Robustness The procedure begins by extracting a subject-specific signature vector ($\tilde{v} \in \mathbb{R}^m$) and enforcing a finite, one-dimensional array structure. To ensure geometric stability, any non-finite entries are mapped to $\{0, \pm 1\}$ and the vector is normalized to unit length. The pipeline implements a hardened loader to align the signature dimension (sig_dim) with the target hidden size (d_{hidden}) of the selected layer. Discrepancies are handled via two strategies in the: **truncation** if $sig_dim > d_{hidden}$, or either **zero-padding** or **interpolation-based padding** if $sig_dim < d_{hidden}$.

Capsule Export and Persistence Each suppression operator (as shown in 3.3) is exported as a lightweight, device-consistent artifact. The capsule registers the normalized suppression direction (d) as a fixed buffer and the scaling factor (α) as a parameter to ensure they are saved and restored with the model state. The exported artifact contains:

- Subject-specific metadata and target layer indices.
- The unit-norm signature vector used to construct d .
- The adapter type, hyperparameters, and the complete state dictionary (including α).

Concrete example. Table 9 shows a compact summary of a serialized capsule. We include these basic statistics (effect size, range, and a short prefix of the vector) as a quick integrity check that the stored signature is well-formed and consistent across export/import.

B.4 Self Healing Loop

Hyperparameters. For reproducibility, Table 10 collects the exact values used in the Self-Healing Loop, grouped by (i) capsule triggering, (ii) LoRA

Metric	Value
Effect Size	2.6197
Dimensions	(4096,)
Min/Max/Mean	-0.0256 / 0.0262 / 0.0001
First 5 Values	[-0.0201, 0.0196, -0.0190, -0.0045, -0.0188]

Table 9: **Example exported capsule summary (Ariana Grande).** Summary statistics of the stored signature direction and metadata.

distillation settings, and (iii) composite objective weights.

Component	Hyperparameters (values)
<i>Capsule trigger</i>	
Soft z -gate (trigger)	$\tau = 3.0; k = 1.6;$
<i>LoRA distillation (global adapter)</i>	
LoRA targets	v_proj, o_proj, q_proj .
LoRA config	$r = 4; \alpha_{LoRA} = 8; \text{dropout} = 0.05; \text{bias} = \text{none}$.
<i>Composite objective (Self-Healing Loop)</i>	
DPO	$\beta = 0.02; w = 1$.
Unlikelihood (factual)	$\lambda_{UL} = 0.03$.
Name-token Unlikelihood (refusal path)	$\lambda_{NTUL} = 0.02; \text{name-token set size} \leq 12$.
Stability regularization	$\lambda_{KL} = 0.03; \lambda_{EWC} = 5.0; \text{Fisher retain pool} \approx 800 \text{ benign prompts}$.

Table 10: **Self-Healing Loop hyperparameters.** Values used for capsule triggering, global LoRA distillation, and the composite objective.

C Additional Results and Ablations

C.1 Signature Validation

The metrics used for Signature validation collectively ensure that the system can accurately detect and suppress forbidden knowledge. The **AUC-ROC** measures how effectively the signature distinguishes between “leak” activations and “control” activations. The **PR-AUC** complements this by addressing class imbalance, demonstrating precision in identifying rare “leak” instances. The **EER (Equal Error Rate)** identifies the optimal threshold for classification, with a low value indicating a highly robust classifier. **Cohen’s d** quantifies the standardized difference between the two score distributions, with a large effect size confirming a statistically significant separation. Finally, the **SNR (Signal-to-Noise Ratio)** evaluates the clarity of the signature against background noise.

Table 11 shows that later MLP layers yield near-perfect discrimination between leak and control activations ($AUC-ROC \approx 1.0$, $EER \approx 0$) with very

Layer	AUC-ROC [CI]	PR-AUC	EER	τ @ 1% FPR	TPR @ 1% FPR	Cohen's d	SNR	Samples
layer.30.mlp	0.996 [0.995, 0.998]	0.991	0.021	1.951	0.956	3.695	3.721	2439/9162
layer.29.mlp	1.000 [1.000, 1.000]	0.999	0.003	0.476	1.000	4.633	4.978	2439/9162
layer.28.mlp	1.000 [1.000, 1.000]	0.999	0.000	0.037	1.000	5.369	7.107	2439/9162
layer.27.mlp	1.000 [1.000, 1.000]	0.999	0.000	0.272	1.000	5.811	7.489	2439/9162
layer.26.mlp	1.000 [1.000, 1.000]	0.999	0.000	0.347	1.000	5.336	6.503	2439/9162
⋮								
layer.4.mlp	0.998 [0.998, 0.999]	0.994	0.017	0.137	0.973	4.533	5.830	2439/9162
layer.3.mlp	0.999 [0.999, 0.999]	0.996	0.011	0.093	0.989	4.425	5.157	2439/9162
layer.2.mlp	1.000 [1.000, 1.000]	0.999	0.000	0.032	1.000	5.668	8.788	2439/9162
layer.1.mlp	0.570 [0.555, 0.581]	0.278	0.439	70.813	0.037	0.208	0.209	2439/9162
layer.0.mlp	0.656 [0.642, 0.667]	0.361	0.361	0.987	0.050	0.580	0.598	2439/9162

Table 11: Layer-wise signature evaluation metrics for the target subject. The results demonstrate near-perfect separability ($AUC \approx 1.0$) in mid-to-late layers, confirming a strong, linearly accessible knowledge signature. Performance degrades in the earliest layers as expected.

large effect sizes (Cohen's $d > 5$ in several layers), indicating a highly separable signature subspace. In contrast, early layers show substantially weaker separability, consistent with lower-level lexical processing dominating early representations.

C.2 Few-shot capability retention

While Table 2 reports zero-shot retention, we additionally verify that the adapter does not degrade performance when tasks include in-context exemplars. We evaluate a representative subset of the benchmarks under their standard few-shot settings (shots shown in Table 12). For each benchmark, we use the same prompt template and the same fixed set of exemplars for both the pre- (Base) and post- (Adapter) model, and score answers via log-likelihood (label-likelihood for ARC/OpenBookQA; option-text likelihood for HellaSwag/WinoGrande), matching our zero-shot evaluation protocol.

Benchmark	Shots	Metric	Pre (Base)	Post (Adapter)	Delta
ARC-Challenge	25	acc_char	78.16	78.50	+0.34
OpenBookQA	8	acc_char	77.40	78.00	+0.60
HellaSwag	10	acc	76.38	76.71	+0.33
WinoGrande	5	acc	71.19	71.35	+0.16

Table 12: **Few-shot capability retention** before and after unlearning (Base vs. Adapter). Shots are benchmark-standard. We report log-likelihood multiple-choice accuracy; **Delta** is Post–Pre.